Tropical Journal of Pharmaceutical Research March 2024; 23 (3): 517-527
ISSN: 1596-5996 (print); 1596-9827 (electronic)

Available online at http://www.tjpr.org
http://dx.doi.org/10.4314/tjpr.v23i3.5

Original Research Article

Investigating the underlying mechanisms of Wuling powder in the management of hyperuricemia based on network pharmacology and molecular docking

Yu Pu[1], Weiguo Li[2], Ying Zhu[3], Haibo Zhou[1]*
[1]Department of Preventive Medicine, [2]Department of Painology, Traditional Chinese Medicine Hospital, [3]Tongliang Center for Disease Control and Prevention, Tongliang, Chongqing 402560, China

For correspondence:* ***Email:* *t_54a@163.com*

Sent for review: 19 September 2023 *Revised accepted: 29 February 2024*

Abstract

Purpose: *To investigate the potential targets and mechanisms of Wuling powder in the treatment of hyperuricemia.*
Methods: *Traditional Chinese Medicine Systems Pharmacy and Analysis Platform (TCMSP) database was used to obtain active compounds and potential targets of Wuling powder. Gene Cards database was searched for hyperuricemia-related targets. Protein interaction networks (PPI) based on intersection targets were created to investigate the relationship between components and disease. Gene ontology (GO), Kyoto gene and genome database (KEGG), and pathway enrichment analysis of intersection targets were performed on the DAVID website to investigate distributed pathways of targets, Using AutoDockTools 1.5.6 software, a molecular docking analysis of core active compounds and core targets was performed to investigate binding status.*
Results: *The study produced 88 active compounds and 598 action targets, including 10 core components and 4 core targets. Targets were mostly enriched in biological processes like apoptosis, protein synthesis, and energy metabolism, all of which were linked to cancer pathways, PI3K-Akt, human cytomegalovirus infection, lipid, atherosclerosis and other signaling pathways. During molecular docking of core components and core targets, favorable binding interactions were observed.*
Conclusion: *The therapeutic potential of Wuling powder against hyperuricemia is achieved by modulating critical biological processes like lipid metabolism, inflammatory responses, and cell apoptosis through a multi-component, multi-target, and multi-pathway approach. This study provides a foundational framework and novel insight for further in-depth investigation into the role of Wuling powder in hyperuricemia treatment.*

Keywords: *Wuling powder, Hyperuricemia, Network pharmacology, Molecular docking, Mechanism*

Tropical Journal of Pharmaceutical Research is indexed by Science Citation Index (SciSearch), Scopus, Web of Science, Chemical Abstracts, Embase, Index Copernicus, EBSCO, African Index Medicus, JournalSeek, Journal Citation Reports/Science Edition, Directory of Open Access Journals (DOAJ), African Journal Online, Bioline International, Open-J-Gate and Pharmacy Abstracts

INTRODUCTION

Hyperuricemia (HUA) is characterized by an imbalance in purine metabolism leading to a systemic metabolic disorder. This condition results in persistent elevation of uric acid levels, caused by an impaired equilibrium between uric acid production and excretion [1]. Hyperuricemia

is the physical and chemical basis of the pathogenesis of gout and is also considered a risk factor for hyperlipidemia, chronic kidney disease, diabetes and cardiovascular disease, posing a serious threat to human health [2].

At present, drugs used to reduce uric acid levels include allopurinol and phenylbromarone [3]. However, long-term use leads to adverse reactions, such as damage to liver and kidney function, gastrointestinal discomfort or skin allergies, and users are prone to withdrawal reactions [4]. As a result, it is expedient to investigate the pathogenesis of hyperuricemia and develop safe and effective therapeutic drugs. Traditional Chinese medicine (TCM) has many advantages in the prevention and treatment of hyperuricemia, such as individualized syndrome differentiation, multiple targets and fewer side effects [5]. Furthermore, TCM has been proven to be safe and effective in treating hyperuricemia by clearing heat and removing dampness [6].

Wuling powder is a representative prescription for clearing dampness and promoting diuresis. A large number of studies have reported that it has certain therapeutic effects on ascites, diabetes nephropathy, osteoporosis and depression [7,8]. Wuling powder is composed of nine traditional Chinese medicines namely *Atractylodes macrocephala*, Plantain herb, *Poria cocos*, *Cistanches herba, Cinnamomi ramulus, Cornus, Radix clematidis, Alisma orientale* and *Anemarrhenae rhizoma*.

It was first prepared by Ding *et al* [9] to reduce hyperuricemia in mice by enhancing renal function and uric acid excretion, while its precise mechanism is yet unknown. Depending on the symptoms of patients with hyperuricemia in this study, drugs were appropriately added or subtracted based on network pharmacology and molecular docking.

This study aimed to investigate the possible targets and processes of Wuling powder's addition and reduction formula in the treatment of hyperuricemia.

METHODS

In searching and identifying Wuling powder's active ingredients, The Traditional Chinese Medicine Systems Pharmacy and Analysis Platform (TCMSP, http://tcmspw.com/tcmsp.php) was utilized to acquire active components. Criteria for selection were oral bioavailability (OB) ≥ 30 % and drug-like characteristics (DL) ≥ 0.18 [10]. The SMILES of active ingredients were obtained utilizing their CAS numbers in the organic small molecule bioactivity database (PubChem, https://pubchem.ncbi.nlm.nih.gov/), which were submitted to Swiss Target Prediction (http://www.swisstargetprediction.ch) under the category of *Homo sapiens* to access the predicted potential targets of Wuling powder. Protein names of targets were converted to corresponding gene names through the UniProt database (https://www.uniprot.org/), and Cytoscape 3.8.0 software was utilized to build the network of Wuling powder's active ingredients and their corresponding targets.

Prediction of disease targets of hyperuricemia

The keyword "hyperuricemia" was searched in the GeneCards database (https://www.genecards.org/) and Online Mendelian Inheritance in Man (OMIM) database (http://www.omim.org), and disease targets were obtained after merging and removing duplicate genes.

Determination of the core components of Wuling powder

Intersection targets between drugs and diseases were acquired using the online Venn diagrams website (http://www.bioinformatics.com.cn/static/others/jvenn/) after eliminating any duplicate targets. These targets were then loaded into the Cytoscape 3.8.0 program to generate a network diagram that shows how active compounds and intersecting targets interact. The top 10 active compounds with the greatest degree values were determined to be the fundamental components.

Building the network of protein-protein interactions

The STRING database (https://string-db.org/) was updated with intersection targets and the multiple proteins tool was chosen. *Homo sapiens* was defined as the organism, the confidence level was set to the greatest possible value (0.900), and free nodes were hidden before the PPI network was displayed.

Identifying primary objectives

The PPI network's file was loaded into Cytoscape 3.8.0 software to carry out topology analysis. To do this, the cytoHubba plugin was used. By arranging target points from inner to outer and adjusting the color from dark to light, the degree value indicated a decreasing trend from high to low. Core targets were determined as those with a degree value ≥ 20.

GO and KEGG enrichment analysis

The intersection targets were uploaded to the Kyoto Encyclopedia of Genes and Genomes (KEGG) and Gene Ontology (GO) enrichment analysis databases on the DAVID database (https://david.ncifcrf.gov/). The GO analysis comprised three categories; biological process (BP), cellular component (CC), and molecular function (MF). Findings of the GO enrichment analysis were visualized using Image GP (http://www.ehbio.com/ImageGP/) to create bubble charts based on the number of enriched targets with $p < 0.05$, while the KEGG enrichment analysis results were displayed in Excel.

Molecular docking analysis

The TCMSP database provided the 2D structure diagrams of core components, while the RCSB PDB database (https://www.rcsb.org/) provided the 3D structure diagrams of core targets. AutoDockTools-1.5.7 software was used for the receptor (dehydration and hydrogenation of core targets) and ligand preparation (hydrogenation of core components). Thereafter, PBDGT format files were saved. The binding energy was calculated by performing docking of the receptor and ligand. Subsequently, the PyMOL software was employed to visualize the results by importing the PBDGT file.

RESULTS

The active components and potential targets of Wuling powder based on retrieval of nine herbs in the TCMSP database include 55 active compounds from *Atractylodes macrocephala*, 70 from Plantain herb, 34 from *Poria cocos*, 75 from *Cistanches herba*, 220 from *Cinnamomi ramulus*, 226 from *Cornus*, 57 from *Radix clematidis*, 46 from *Alisma orientale* and 81 from *Anemarrhenae rhizoma*. After screening with OB ≥ 30 % and DL ≥ 0.18; 7 active compounds from *Atractylodes macrocephala*, 10 from Plantain herb, 15 from *Poria cocos*, 6 from *Cistanches herba*, 7 from *Cinnamomi ramulus*, 20 from *Cornus*, 7 from *Radix clematidis*, 10 from *Alisma orientale* and 15 from *Anemarrhenae rhizoma* were obtained. After removing duplicate values, a total of 88 active compounds of Wuling powder were acquired (Table 1). There were 2846 corresponding targets, which were standardized by the UniProt database, and 598 effective targets were ultimately determined by removing invalid and duplicate targets. Network among drugs, active ingredients and targets was constructed (Figure 1).

Core components of *Wuling* powder

Utilizing the GeneCards and Online Mendelian Inheritance in Man (OMIM) databases, 878 hyperuricemia-related disease targets were identified. A total of 122 potential targets were determined by using Venn diagram (Figure 2 A). The network between active ingredients and intersection targets was constructed (Figure 2 B), in which the degree value of the node was proportional to its shape size. Primary constituents were considered to be the top ten active compounds with the degree value (Table 1), including quercetin, baicalin, dihydroxyl phthalate, asperglaude, poricoic acid B, poricoic acid C, 7,9(11)-dehydropachymic acid, poricoic acid A, eburicoic acid, and dehydroebricic acid.

Core targets of Wuling powder in the treatment of hyperuricemia

To identify the interaction relationship between these predicted targets, a protein-protein interaction network diagram was drawn (Figure 3 A). The network comprised 122 nodes and 307 edges, exhibiting an average degree value of 5.03. Topology analysis results are shown in Figure 3B, in which the degree value of the node was directly proportional to the color depth. Targets with a degree value ≥ 20 were determined as core targets including TP53, RELA, MAPK1, and TNF respectively (Table 2).

Gene ontology enrichment analysis of intersection targets

To investigate the mechanism of Wuling powder in hyperuricemia, gene ontology (GO) enrichment analysis was performed on 122 overlapping targets. The findings demonstrated that a total of 806 elements were classified into 105 molecular functions, 50 cell components, and 651 biological activities. A bubble chart showed the top 20 products with enhanced goal numbers in each category (Figure 4). In the category of biological process, targets were mainly enriched in the following functions, including negative regulation of the apoptotic process, positive regulation of transcription from RNA polymerase II promoter, response to xenobiotic stimulus and apoptotic process. For the cellular component category, targets were mainly enriched in the cytoplasm, cytosol, nucleus, plasma membrane and nucleoplasm. In molecular function, targets were mainly enriched in protein binding, identical protein binding, protein homodimerization activity, ATP binding, and other functions. The results suggested that Wuling powder might play a therapeutic role in.

Table 1: Drug-active compound information

Drug	Abbreviation	Compound	Compound name
Atractylodes Macrocephala koidz.	BZ	BZ1	12-senecioyl-2E,8E,10E-atractylentriol
Atractylodes Macrocephala koidz.	BZ	BZ2	14-acetyl-12-senecioyl-2E,8E,10E-atractylentriol
Atractylodes Macrocephala koidz.	BZ	BZ3	14-acetyl-12-senecioyl-2E,8Z,10E-atractylentriol
Atractylodes Macrocephala koidz.	BZ	BZ4	α-Amyrin
Atractylodes Macrocephala koidz.	BZ	BZ5	(3S,8S,9S,10R,13R,14S,17R)-10,13-dimethyl-17-((2R,5S)-5-propan-2-yloctan-2-yl)-2,3,4,7,8,9,11,12,14,15,16,17-dodecahydro-1H-cyclopenta(a)phenanthren-3-ol
Atractylodes Macrocephala koidz.	BZ	BZ6	3β-acetoxyatractylone
Atractylodes Macrocephala koidz.	BZ	BZ7	8β-ethoxy atractylenolide Ⅲ
Plantain herb	CQC	CQC1	luteolin
Plantain herb	CQC	CQC2	Dinatin
Plantain herb	CQC	CQC3	baicalein
Plantain herb	CQC	CQC4	Baicalin
Plantain herb	CQC	CQC5	6-OH-Luteolin
Plantain herb	CQC	CQC6	melampyroside
Plantain herb	CQC	CQC7	stigmasteryl palmitate
Plantain herb	CQC	CQC8	β-sitosteryl palmitate
Plantain herb	CQC	A1	sitosterol
Plantain herb	CQC	B1	Stigmasterol
Poria cocos (Schw.) Wolf.	FL	FL1	(2R)-2-((3S,5R,10S,13R,14R,16R,17R)-3,16-dihydroxy-4,4,10,13,14-pentamethyl-2,3,5,6,12,15,16,17-octahydro-1H-cyclopenta(a)phenanthren-17-yl)-6-methylhept-5-enoic acid
Poria cocos (Schw.) Wolf.	FL	FL2	trametenolic acid
Poria cocos (Schw.) Wolf.	FL	FL3	7,9(11)-dehydropachymic acid
Poria cocos (Schw.) Wolf.	FL	FL4	Cerevisterol
Poria cocos (Schw.) Wolf.	FL	FL5	(2R)-2-((3S,5R,10S,13R,14R,16R,17R)-3,16-dihydroxy-4,4,10,13,14-pentamethyl-2,3,5,6,12,15,16,17-octahydro-1H-cyclopenta(a)phenanthren-17-yl)-5-isopropyl-hex-5-enoic acid
Poria cocos (Schw.) Wolf.	FL	FL6	ergosta-7,22E-dien-3beta-ol
Poria cocos (Schw.) Wolf.	FL	FL7	Ergosterol peroxide
Poria cocos (Schw.) Wolf.	FL	FL8	(2R)-2-((5R,10S,13R,14R,16R,17R)-16-hydroxy-3-keto-4,4,10,13,14-pentamethyl-1,2,5,6,12,15,16,17-octahydrocyclopenta(a)phenanthren-17-yl)-5-isopropyl-hex-5-enoic acid
Poria cocos (Schw.) Wolf.	FL	FL9	3beta-Hydroxy-24-methylene-8-lanostene-21-oic acid
Poria cocos (Schw.) Wolf.	FL	FL10	pachymic acid
Poria cocos (Schw.) Wolf.	FL	FL11	Poricoic acid A
Poria cocos (Schw.) Wolf.	FL	FL12	Poricoic acid B
Poria cocos (Schw.) Wolf.	FL	FL13	Poricoic acid C
Poria cocos (Schw.) Wolf.	FL	FL14	hederagenin
Poria cocos (Schw.) Wolf.	FL	FL15	dehydroburicoic acid
Cistanches herba	GHRCR	GHRCR1	quercetin
Cistanches herba	GHRCR	GHRCR2	arachidonate
Cistanches herba	GHRCR	GHRCR3	suchilactone
Cistanches herba	GHRCR	GHRCR4	Yangambin
Cistanches herba	GHRCR	GHRCR5	Marckine
Cistanches herba	GHRCR	C1	beta-sitosterol
Cinnamomi ramulus	GZ	GZ1	ent-Epicatechin
Cinnamomi ramulus	GZ	GZ2	(+)-catechin
Cinnamomi ramulus	GZ	GZ3	(-)-taxifolin
Cinnamomi ramulus	GZ	GZ4	taxifolin
Cinnamomi ramulus	GZ	GZ5	Peroxyergosterol
Cinnamomi ramulus	GZ	A1	sitosterol
Cinnamomi ramulus	GZ	C1	beta-sitosterol
Cinnamomi ramulus	GZ	GZ1	ent-Epicatechin
Cinnamomi ramulus	GZ	GZ2	(+)-catechin
Cinnamomi ramulus	GZ	GZ3	(-)-taxifolin

Table 1: Drug-active compound information (*continued*)

Drug	Abbreviation	Compound	Compound name
Cinnamomi ramulus	GZ	GZ4	taxifolin
Cinnamomi ramulus	GZ	GZ5	Peroxyergosterol
Cinnamomi ramulus	GZ	A1	sitosterol
Cinnamomi ramulus	GZ	C1	beta-sitosterol
Cornus officinalis Sieb. Et Zucc.	SYR	SYR1	gallic acid-3-O-(6'-O-galloyl)-glucoside
Cornus officinalis Sieb. Et Zucc.	SYR	SYR2	Mandenol
Cornus officinalis Sieb. Et Zucc.	SYR	SYR3	Ethyl linolenate
Cornus officinalis Sieb. Et Zucc.	SYR	SYR4	poriferast-5-en-3beta-ol
Cornus officinalis Sieb. Et Zucc.	SYR	SYR5	Diop
Cornus officinalis Sieb. Et Zucc.	SYR	SYR6	Ethyl oleate (NF)
Cornus officinalis Sieb. Et Zucc.	SYR	SYR7	Leucanthoside
Cornus officinalis Sieb. Et Zucc.	SYR	SYR8	malkangunin
Cornus officinalis Sieb. Et Zucc.	SYR	SYR9	2,6,10,14,18-pentamethylicosa-2,6,10,14,18-pentaene
Cornus officinalis Sieb. Et Zucc.	SYR	SYR10	3,4-Dehydrolycopen-16-al
Cornus officinalis Sieb. Et Zucc.	SYR	SYR11	3,6-Digalloylglucose
Cornus officinalis Sieb. Et Zucc.	SYR	SYR12	Cornudentanone
Cornus officinalis Sieb. Et Zucc.	SYR	SYR13	Hydroxygenkwanin
Cornus officinalis Sieb. Et Zucc.	SYR	SYR14	Telocinobufagin
Cornus officinalis Sieb. Et Zucc.	SYR	SYR15	gemin D
Cornus officinalis Sieb. Et Zucc.	SYR	SYR16	lanosta-8,24-dien-3-ol,3-acetate
Cornus officinalis Sieb. Et Zucc.	SYR	SYR17	Tetrahydroalstonine
Cornus officinalis Sieb. Et Zucc.	SYR	A1	sitosterol
Cornus officinalis Sieb. Et Zucc.	SYR	B1	Stigmasterol
Cornus officinalis Sieb. Et Zucc.	SYR	C1	beta-sitosterol
Radix clematidis	WLX	WLX1	(4aS,6aR,6aS,6bR,8aR,10R,12aR,14bS)-10-hydroxy-2,2,6a,6b,9,9,12a-heptamethyl-1,3,4,5,6,6a,7,8,8a,10,11,12,13,14b-tetradecahydropicene-4a-carboxylic acid
Radix clematidis	WLX	WLX2	(6Z,10E,14E,18E)-2,6,10,15,19,23-hexamethyltetracosa-2,6,10,14,18,22-hexaene
Radix clematidis	WLX	WLX3	ClematosideA'_qt
Radix clematidis	WLX	WLX4	Embinin
Radix clematidis	WLX	WLX5	Diheptyl phthalate
Radix clematidis	WLX	A1	sitosterol
Radix clematidis	WLX	B1	Stigmasterol
Alisma orientale (Sam.) Juz.	YZX	YZX1	sitosterol
Alisma orientale (Sam.) Juz.	YZX	YZX2	Alisol B
Alisma orientale (Sam.) Juz.	YZX	YZX3	Alisol B monoacetate
Alisma orientale (Sam.) Juz.	YZX	YZX4	alisol,b,23-acetate
Alisma orientale (Sam.) Juz.	YZX	YZX5	16β-methoxyalisol B monoacetate
Alisma orientale (Sam.) Juz.	YZX	YZX6	alisol B
Alisma orientale (Sam.) Juz.	YZX	YZX7	alisol C
Alisma orientale (Sam.) Juz.	YZX	YZX8	alisol C monoacetate
Alisma orientale (Sam.) Juz.	YZX	YZX9	((1S,3R)-1-((2R)-3,3-dimethyloxiran-2-yl)-3-((5R,8S,9S,10S,11S,14R)-11-hydroxy-4,4,8,10,14-pentamethyl-3-oxo-1,2,5,6,7,9,11,12,15,16-decahydrocyclopenta(a)phenanthren-17-yl) butyl) acetate
Alisma orientale (Sam.) Juz.	YZX	A1	1-Monolinolein
Anemarrhenae rhizoma	YZM	YZM1	kaempferol
Anemarrhenae rhizoma	YZM	YZM2	(Z)-3-(4-hydroxy-3-methoxy-phenyl)-N-(2-(4-hydroxyphenyl)ethyl)acrylamide
Anemarrhenae rhizoma	YZM	YZM3	diosgenin
Anemarrhenae rhizome	YZM	YZM4	coumaroyltyramine
Anemarrhenae rhizome	YZM	YZM5	asperglaucide
Anemarrhenae rhizome	YZM	YZM6	Mangiferolic acid
Anemarrhenae rhizome	YZM	YZM7	Anhydroicaritin
Anemarrhenae rhizome	YZM	YZM8	Anemarsaponin F_qt
Anemarrhenae rhizome	YZM	YZM9	Chrysanthemaxanthin
Anemarrhenae rhizome	YZM	YZM10	Hippeastrine
Anemarrhenae rhizome	YZM	YZM11	Timosaponin B III_qt
Anemarrhenae rhizoma	YZM	YZM12	Icariin I
Anemarrhenae rhizoma	YZM	YZM13	Anemarsaponin C_qt
Anemarrhenae rhizoma	YZM	YZM14	Anemarsaponin E_qt
Anemarrhenae rhizoma	YZM	B1	Stigmasterol

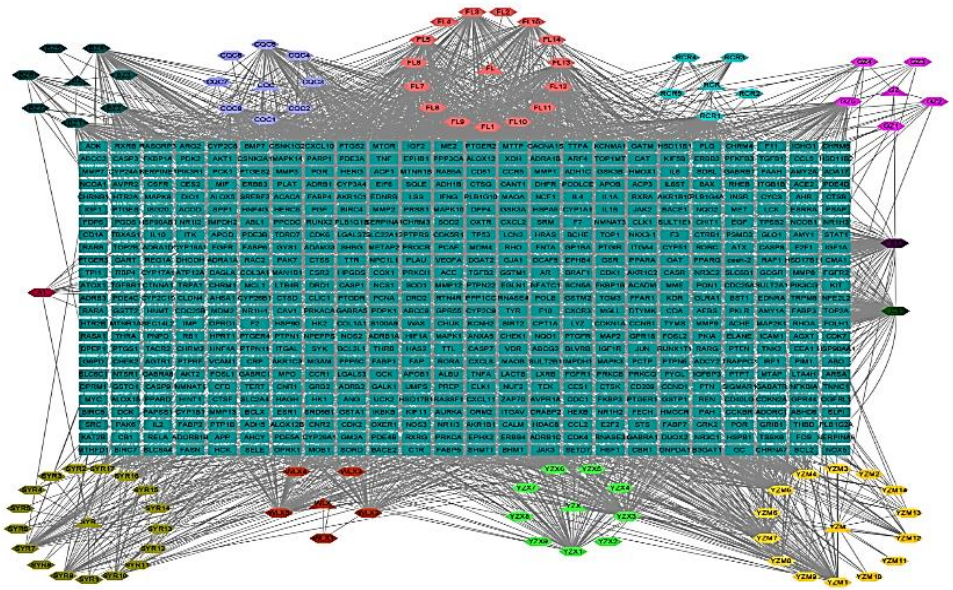

Figure 1: Drug-active ingredient-target network. Triangles represent herbs, hexagons represent active ingredients, and rectangles represent targets

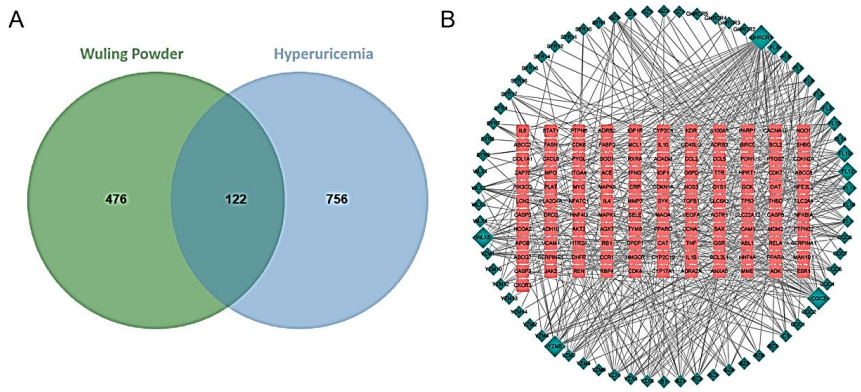

Figure 2: Core components of Wuling powder in the treatment of hyperuricemia. (A) Venn diagram of intersection targets. Green represents Wuling powder, and blue represents hyperuricemia. (B) Target network with active ingredient intersection. Intersection targets are represented by squares, while the active components are symbolized by diamonds. As the degree value rises, the shape's size grows

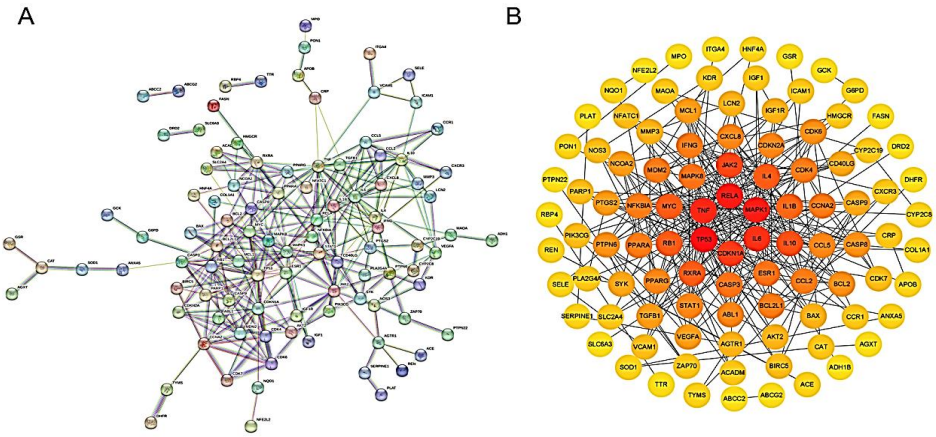

Figure 3: Core targets of Wuling powder in the treatment of hyperuricemia. (A) Protein-protein interaction network diagram was acquired from the STRING database. With 307 edges and 122 nodes, its average degree value is 5.03. (B) Topology analysis performed by Cytoscape. Color depth and arrangement position of nodes are proportional to the degree value

Table 2: Core compound information

Compound	Compound name	Degree
GHRCR1	quercetin	50
CQC3	baicalein	27
WLX5	Diheptyl phthalate	20
YZM5	asperglaucide	20
FL12	Poricoic acid B	19
FL13	Poricoic acid C	16
FL3	7,9(11)-dehydropachymic acid	15
FL11	Poricoic acid A	15
FL9	eburicoic acid	15
FL15	dehydroeburicoic acid	15

hyperuricemia by regulating cell apoptosis, protein binding and energy metabolism

Kyoto Encyclopedia of Genes and Genomes (KEGG) enrichment and pathway analysis of intersection targets

The KEGG enrichment analysis was performed to investigate intersection targets. A total of 146 signaling pathways were obtained ($p < 0.05$) and top 20 items of the target number enrichment were presented (Figure 5).

Molecular docking between core components and core targets

All components had certain binding forces with targets. Among them, eburicoic acid exerted strong affinity to all core targets (Table 3), and dehydroeburicoic acid was also closely bound with TP53 and RELA. Visualization analysis was performed on docking results with excellent binding (Figure 6 B).

Eburicoic acid formed hydrogen bonds with amino acid residues GLU-180 and then bound to TP53. Additionally, dehydroeburicoic acid is linked to TP53 via hydrogen bonds with ASN-239 and TYR-107 amino acid residues. Furthermore, dehydroeburicoic acid is linked to RELA via hydrogen bonds with the amino acid residues GLU-17 and TYR-19.

DISCUSSION

Traditional Chinese medicine believes that the etiology of hyperuricemia is mainly due to dysfunction of the spleen and kidney, with dampness, phlegm, turbidity and blood stasis as main indicators [5]. Wuling powder is characterized by heat, and its therapeutic effect on hyperuricemia conforms to the TCM theory that ‘those who suffer from phlegm syndrome should be treated with warm medicine’.

In this study, it was identified that quercetin, baicalin, dihydroxyl phthalate, asperglaude, poricoic acid B, poricoic acid C, 7,9(11)-dehydropachymic acid, poricoic acid A, eburicoic acid, and dehydroebricic acid in *Wuling* powder may be key elements in the treatment of hyperuricemia.

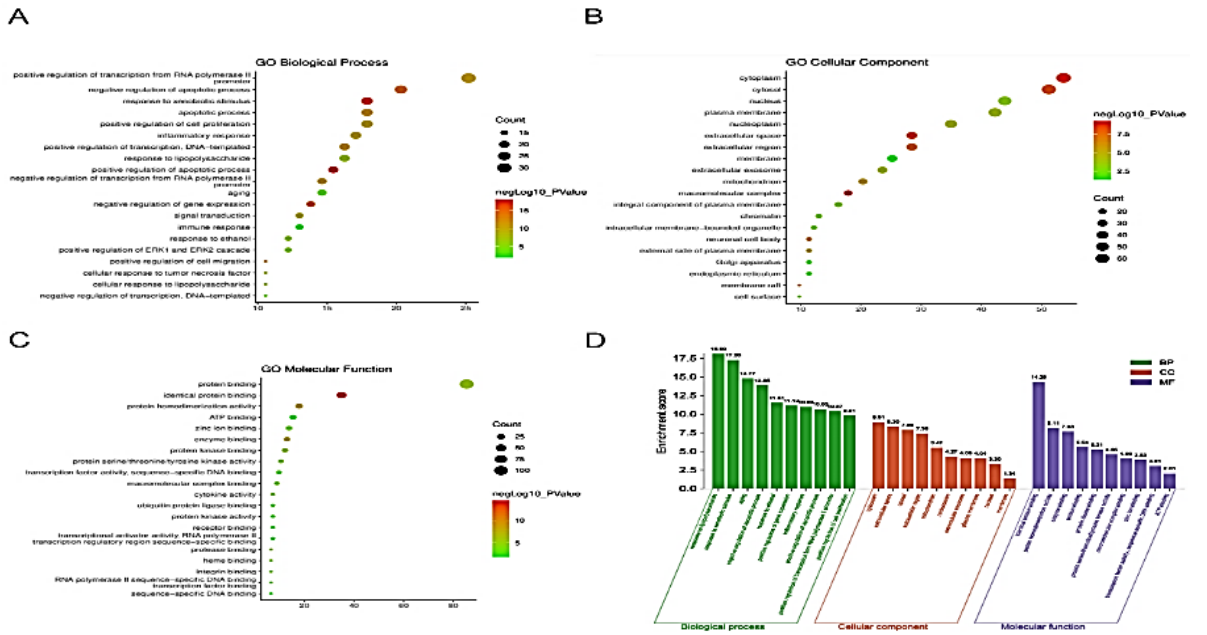

Figure 4: GO enrichment analysis of intersection targets. (A) Bubble charts of cellular component category. (B) Bubble charts of biological process category. (C) Bubble charts of molecular function category. (D) Top ten enrichments in P-value ranking of each category

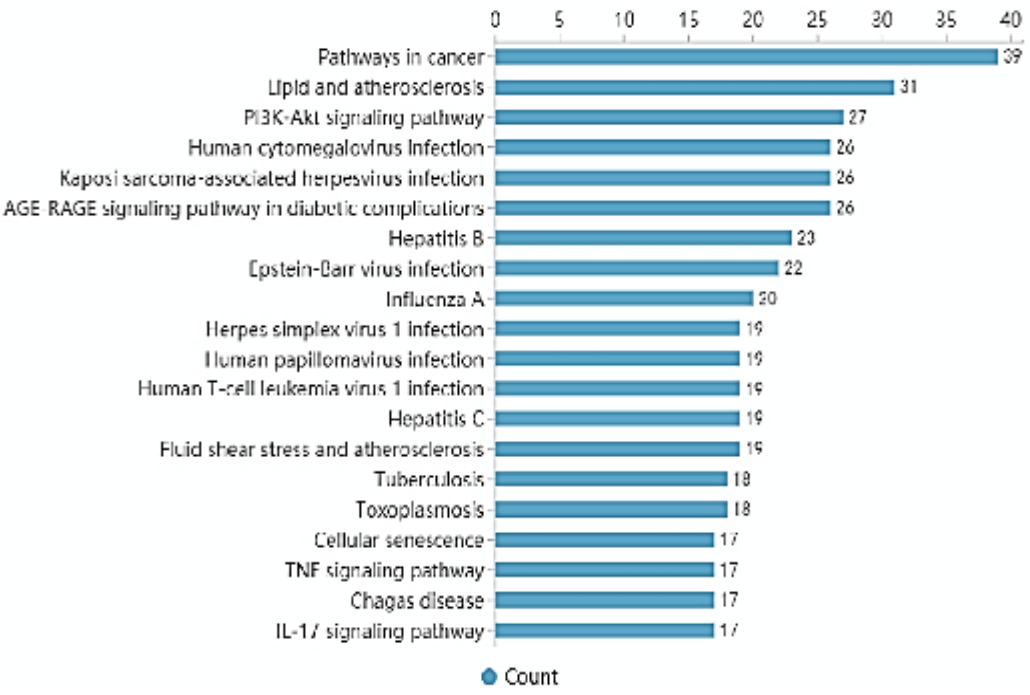

Figure 5: KEGG enrichment analysis of intersection targets. Top 20 pathways with enriched number arrangement

Table 3: Core targets information in the PPI network

Core target	Full Name	Degree
TP53	Cellular tumor antigen p53	28
RELA	Transcription factor p65	21
MAPK1	Mitogen-activated protein kinase 1	21
TNF	Tumor necrosis factor	20

Quercetin possesses anti-inflammatory, antitumor, antioxidant, and metabolic syndrome-ameliorating effects. It has been proven that it does not only reduce uric acid production by acting on xanthine oxidase and other related enzymes, but it also promotes the activity of uric acid excretion transporters to increase uric acid excretion and effectively resist hyperuricemia [12,13]. Baicalein is also an important class of flavonoids. In addition to inhibiting activity of xanthine oxidase, studies have found that it also regulates uric acid transporters (GLUT9 and URAT1) [14]. Dihydroxyl phthalate is a proliferator-activated receptor of peroxisome α (PPARα) agonist. Although there is no study about its effect on hyperuricemia, PPARα, which regulates fatty acid metabolism, has been proven to cause excessive generation of reactive oxygen species, lipid peroxidation, and oxidative damage [15].

Uric acid is an oxidation product of purine metabolism, so reducing oxidation level may have certain effect on reducing generation of uric acid. Asperglaude is believed to be a metabolic product of *Saccharomyces cereus*, which regulates NF-κB and MAPK signaling pathways to exert anti-inflammatory and antitumor effects [16]. Poria cocos has been widely studied in diabetes, kidney and heart diseases. Poricoic acids A, B, and C are the most effective compounds of Poria cocos and effectively improve renal interstitial fibrosis, fat metabolism and other related diseases through AMPK, PPARα and other pathways [17,18]. Eburicoic acid exhibits a strong binding force with all core targets. It inhibits inflammatory response by regulating the PI3K/Akt signaling pathway [19], while inflammation is a key pathological feature of hyperuricemia.

Furthermore, based on the topology of the PPI network, TP53, RELA, MAPK1, and TNF were identified as potential main targets of Wuling powder in the treatment of hyperuricemia. TP53 is a tumor suppressor gene, whose mutations lead to various cancer lesions in different ways [20]. TP53 binds to the promoter of ABCG2 gene, and the degradation of TP53 leads to a decreased expression of ABCG2, which is a risk factor for elevated uric acid [21]. At the same time, uric acid also promotes TP53-mediated autophagy to accelerate adverse progress of hyperuricemia [22].

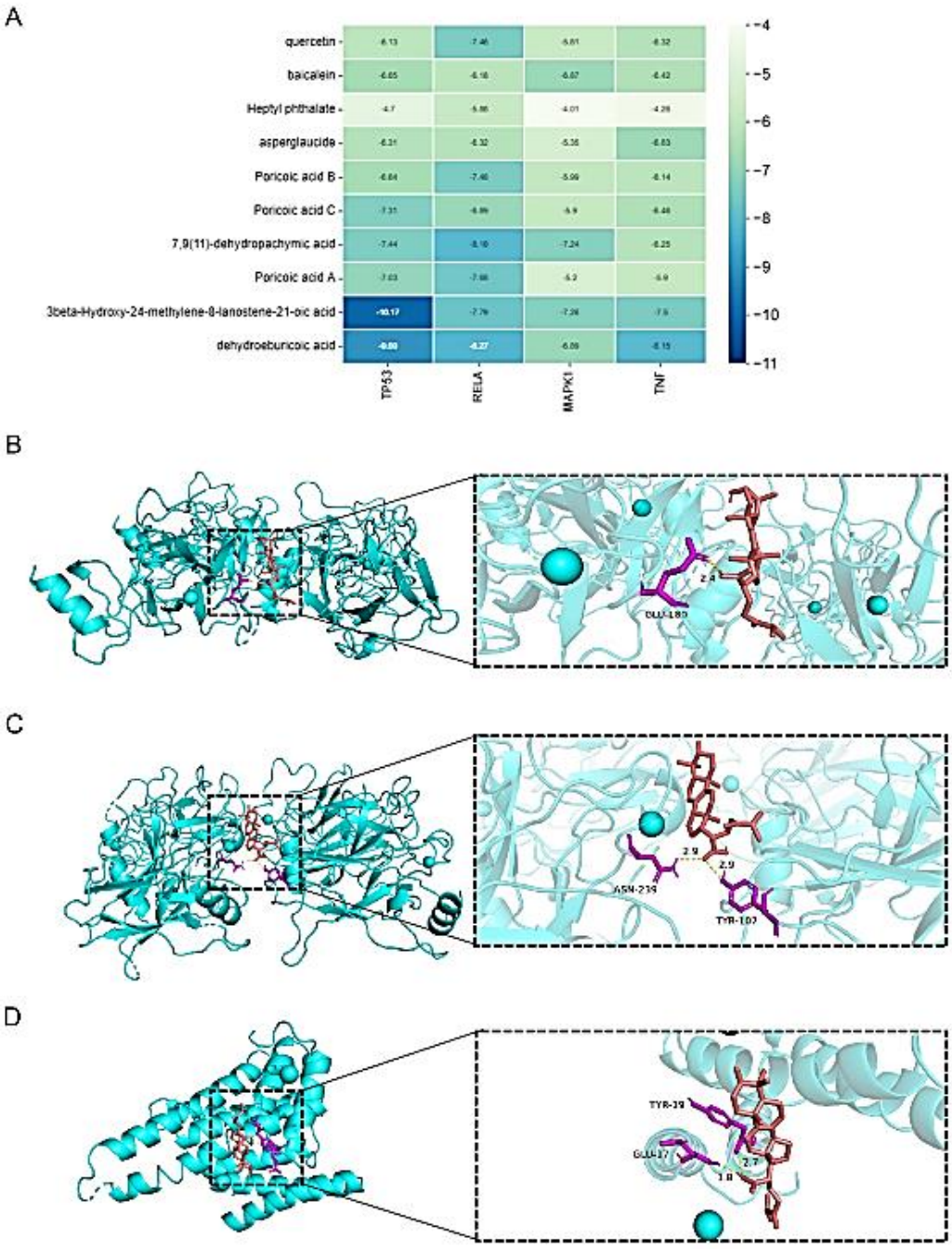

Figure 6: Molecular docking analysis. (A) Minimum binding energy between core component and core target. (B) Molecular docking diagram and binding sites of eburicoic acid and TP53. (C) Molecular docking diagram and binding sites of dehydroeburicoic acid and TP53. (D) Molecular docking diagram and binding sites of dehydroeburicoic acid and RELA

Deamidation of one of NF-κB's subunits, RELA, has been shown to stop NF-κB-mediated pro-inflammatory response [23]. MAPK1 has been widely studied as a target for various malignant tumors, mainly focusing on regulating cell apoptosis, inflammatory response, and autophagy [24]. Tumor necrosis factor (TNF) is a classic pro-inflammatory factor, and its expression is upregulated in hyperuricemia [25]. Through enrichment analysis of targets, it was found that pathways in cancer, PI3K-Akt, human cytomegalovirus infection, lipid and atherosclerosis and other signaling pathways are crucial in the fight against hyperuricemia. In addition, the involved biological processes included apoptosis, lipid peroxidation, inflammatory reaction and energy metabolism. Meanwhile, core targets that were screened are closely related to these signaling pathways. This study further revealed that Wuling powder

resisted hyperuricemia mainly by influencing biological processes such as apoptosis, lipid metabolism and inflammatory reactions.

CONCLUSION

The effectiveness of Wuling powder in treating hyperuricemia is attributed to key constituents including quercetin, baicalein, poricoic acid, and eburicoic acid through the regulation of vital biological processes such as apoptosis, inflammatory response, and lipid metabolism pathways. Furthermore, *Wuling* powder creates stable hydrogen bonds with these main targets through molecular docking. By shedding light on the intricate molecular mechanisms at play, This study provides a foundational framework and novel insight for more in-depth investigation into the role of *Wuling* powder in hyperuricemia treatment.

DECLARATIONS

Acknowledgements

None provided.

Funding

None provided.

Ethical approval

None provided.

Availability of data and materials

The datasets used and/or analyzed during the current study are available from the corresponding author on reasonable request.

Conflict of Interest

No conflict of interest associated with this work.

Contribution of Authors

We declare that this work was done by the authors named in this article and all liabilities pertaining to claims relating to the content of this article will be borne by the authors. Yu Pu and Weiguo Li contributed equally to this work.

Open Access

REFERENCES

1. *Su X, Liu J, Sun N, Huo Y. Hyperuricemia is associated with more cardiometabolic risk factors in hypertensive younger Chinese adults than in elderly. Front Cardiovasc Med 2023; 10: 1133724.*
2. *Sofue T. Hyperuricemia: the third key player for nephrosclerosis with ischemia. Hypertens Res 2023; 46(7): 1707-1709.*
3. *Wu H, Wang Y, Li YL, Huang JJ, Lin ZJ, Zhang B. Current status and trends for natural products on hyperuricemia study: A scientometric visualization analysis from 2000 to 2021. Eur Rev Med Pharmacol 2023; 27(7): 2832-2844.*
4. *Lai SW, Liao KF, Kuo YH, Hwang BF, Liu CS. Comparison of benzbromarone and allopurinol on the risk of chronic kidney disease in people with asymptomatic hyperuricemia. Eur J Intern Med 2023; 113: 91-97.*
5. *Yang L, Wang B, Ma L, Fu P. Traditional Chinese herbs and natural products in hyperuricemia-induced chronic kidney disease. Front Pharmacol 2022; 13: 971032.*
6. *Yu XN, Wu HY, Deng YP, Zhuang GT, Tan BH, Huang YZ, Tang SY, Tu X, Jordan JB, Zhong S. "Yellow-dragon Wonderful-seed Formula" for hyperuricemia in gout patients with dampness-heat pouring downward pattern: a pilot randomized controlled trial. Trials 2018; 19(1): 551.*
7. *Mou Y, Wang X, Wang T, Wang Y, Wang H, Zhao H, Chen Q, Xia L, Zhang Y. Clinical application and pharmacological mechanism of Wuling powder in the treatment of ascites: A systematic review and network pharmacological analysis. Biomed Pharmacother 2022; 146: 112506.*
8. *Yang Y, Sha W, Hou K, Xu Y, Tan S, Yin H, Chen L, Lei T. Efficacy and safety of Wuling powder in the treatment of patients with diabetic nephropathy: A systematic review and meta-analysis. Evid-Based Compl Alt 2022; 2022: 1720749.*
9. *Ding XQ, Pan Y, Wang X, Ma YX, Kong LD. Wuling san ameliorates urate under-excretion and renal dysfunction in hyperuricemic mice. Chin J Nat Med 2013; 11(3): 214-221.*
10. *Xu X, Zhang W, Huang C, Li Y, Yu H, Wang Y, Duan J, Ling Y. A novel chemometric method for the prediction of human oral bioavailability. Int J Mol Sci 2012; 13(6): 6964-6982.*
11. *Di Muzio E, Toti D, Polticelli F. DockingApp: a user-friendly interface for facilitated docking simulations with AutoDock Vina. J Comput Aid Mol Des 2017; 31(2): 213-218.*

12. Zhou J, Zhang Y, Cheng L. Meta-analysis of the effect of losartan relative to other angiotensin receptor antagonists on serum uric acid level. Trop J Pharm Res 2023; 22(9):1999-2008 doi: 10.4314/tjpr.v22i9.31
13. Nutmakul T. A review on benefits of quercetin in hyperuricemia and gouty arthritis. Saudi Pharm J 2022; 30(7): 918-926.
14. Chen Y, Zhao Z, Li Y, Yang Y, Li L, Jiang Y, Lin C, Cao Y, Zhou P, Tian Y, et al. Baicalein alleviates hyperuricemia by promoting uric acid excretion and inhibiting xanthine oxidase. Phytomed 2021; 80: 153374.
15. Jin M, Dewa Y, Kawai M, Nishimura J, Saegusa Y, Kemmochi S, Harada T, Shibutani M, Mitsumori K. Induction of liver preneoplastic foci in F344 rats subjected to 28-day oral administration of diheptyl phthalate and its in vivo genotoxic potential. Toxicol 2009; 264(1-2): 16-25.
16. Tran HT, Gao X, Kretschmer N, Pferschy-Wenzig EM, Raab P, Pirker T, Temml V, Schuster D, Kunert O, Huynh L, et al. Anti-inflammatory and antiproliferative compounds from Sphaeranthus africanus. Phytomed 2019; 62: 152951.
17. Kim JH, Sim HA, Jung DY, Lim EY, Kim YT, Kim BJ, Jung MH. Poria cocus wolf extract ameliorates hepatic steatosis through regulation of lipid metabolism, inhibition of ER stress, and activation of autophagy via AMPK activation. Int J Mol Sci 2019; 20(19): 4801.
18. Chen DQ, Wang YN, Vaziri ND, Chen L, Hu HH, Zhao YY. Poricoic acid A activates AMPK to attenuate fibroblast activation and abnormal extracellular matrix remodeling in renal fibrosis. Phytomed 2020; 72: 153232.
19. Wang J, Zhang P, He H, Se X, Sun W, Chen B, Zhang L, Yan X, Zou K. Eburicoic acid from Laetiporus sulphureus (Bull.:Fr.) Murrill attenuates inflammatory responses by inhibiting LPS-induced activation of PI3K/Akt/mTOR/NF-kappaB pathways in RAW264.7 cells. N-S Arch Pharmacol 2017; 390(8): 845-856.
20. Olivier M, Hollstein M, Hainaut P. TP53 mutations in human cancers: origins, consequences, and clinical use. Csh Perspect Biol 2010; 2(1): a1008.
21. Ristic B, Sivaprakasam S, Narayanan M, Ganapathy V. Hereditary hemochromatosis disrupts uric acid homeostasis and causes hyperuricemia via altered expression/activity of xanthine oxidase and ABCG2. Biochem J 2020; 477(8): 1499-1513.
22. Hu Y, Shi Y, Chen H, Tao M, Zhou X, Li J, Ma X, Wang Y, Liu N. Blockade of autophagy prevents the progression of hyperuricemic nephropathy through inhibiting NLRP3 inflammasome-mediated pyroptosis. Front Immunol 2022; 13: 858494.
23. Zhao J, Tian M, Zhang S, Delfarah A, Gao R, Rao Y, Savas AC, Lu A, Bubb L, Lei X, et al. Deamidation shunts RelA from mediating inflammation to aerobic glycolysis. Cell Metab 2020; 31(5): 937-955.
24. Zhao L, Zhou R, Wang Q, Cheng Y, Gao M, Huang C. MicroRNA-320c inhibits articular chondrocytes proliferation and induces apoptosis by targeting mitogen-activated protein kinase 1 (MAPK1). Int J Rheum Dis 2021; 24(3): 402-410.
25. Yang B, Xin M, Liang S, Huang Y, Li J, Wang C, Liu C, Song X, Sun J, Sun W. Naringenin ameliorates hyperuricemia by regulating renal uric acid excretion via the PI3K/AKT signaling pathway and renal inflammation through the NF-kappaB Signaling Pathway. J Agr Food Chem 2023; 71(3): 1434-1446.